Vibrational Raman Optical Activity of 1-Phenylethanol and 1-Phenylethylamine: Revisiting Old Friends

JOSEF KAPITÁN,[1] CHRISTIAN JOHANNESSEN,[1] PETR BOUŘ,[2] LUTZ HECHT,[1] AND LAURENCE D. BARRON[1]*
[1]*WestChem, Department of Chemistry, University of Glasgow, Glasgow, United Kingdom*
[2]*Institute of Organic Chemistry and Biochemistry, Academy of Sciences, Flemingovo nám., Prague, Czech Republic*

Contribution to the special thematic project "Advances in Chiroptical Methods"

ABSTRACT The samples used for the first observations of vibrational Raman optical activity (ROA) in 1972, namely both enantiomers of 1-phenylethanol and 1-phenylethylamine, have been revisited using a modern commercial ROA instrument together with state-of-the-art ab initio calculations. The simulated ROA spectra reveal for the first time the vibrational origins of the first reported ROA signals, which comprised similar couplets in the alcohol and amine in the spectral range ~280–400 cm^{-1}. The results demonstrate how easy and routine ROA measurements have become, and how current ab initio quantum–chemical calculations are capable of simulating experimental ROA spectra quite closely provided sufficient averaging over accessible conformations is included. Assignment of absolute configuration is, inter alia, completely secure from results of this quality. Anharmonic corrections provided small improvements in the simulated Raman and ROA spectra. The importance of conformational averaging emphasized by this and previous related work provides the underlying theoretical background to ROA studies of dynamic aspects of chiral molecular and biomolecular structure and behavior. *Chirality 21:S4–S12, 2009.*

"We shall not cease from exploration, and the end of all our exploring will be to arrive where we started and know the place for the first time."

T. S. Eliot (Four Quartets)

KEY WORDS: vibrational optical activity; ab initio calculations; Raman optical activity; solution conformation; absolute configuration

INTRODUCTION

Amid much controversy, the first genuine measurements of Raman optical activity (ROA), which constituted the first observations of vibrational optical activity in typical relatively small chiral molecules in the liquid phase, were reported over 35 yrs ago[1] and confirmed a few years later.[2] The compounds studied were the two enantiomers of 1-phenylethanol and 1-phenylethylamine, the structures of the (+)-(*R*)-enantiomers of which are displayed in Figure 1. Depolarized ROA spectra were measured in right-angle scattering within the spectral range ~280–400 cm^{-1}, where similar couplets (referred to here as the "BBB couplets" after the authors of the first report[1]) were observed in the alcohol and amine with equal and opposite signs for each pair of enantiomers. The intervening years have witnessed immense progress both in the measurement of ROA spectra and in their theoretical interpretation.[3,4] A vast range of chiral molecular species, from small organic molecules to intact viruses, may now be measured routinely,[4] with reliable ab initio quantum–chemical simulations providing complete solution structures (conformation and absolute configuration) of smaller chiral molecules and oligomers[5–8] (see these articles for many more references).

The original observations[1,2] used the incident circular polarization (ICP) measurement strategy in the form of a small difference in the Raman-scattered intensity in right- and left-circularly polarized incident light. In this article, we revisit the same four samples and present high-quality spectra acquired using a commercial ROA instrument, which employs the alternative scattered circular polarization (SCP) strategy, in which the intensity of a small circularly polarized component in the scattered light is measured using incident light of fixed polarization. In the far-from-resonance approximation, which obtains for this study, ICP and SCP measurements provide equivalent results.[9] The ROA spectra are simulated using state-of-the-art calculations which, inter alia, reveal for the first time the vibrational

Contract grant sponsor: U.K. Engineering and Physical Sciences Research Council; Contract grant number: EP/F029713/1.
Contract grant sponsor: Grant Agency of the Czech Academy of Science; Contract grant number: A4005507020.
*Correspondence to: Laurence D. Barron, Department of Chemistry, University of Glasgow, Glasgow G12 8QQ, United Kingdom.
E-mail:laurence@chem.gla.ac.uk
Received for publication 25 March 2009; Accepted 23 April 2009
DOI: 10.1002/chir.20747
Published online 18 June 2009 in Wiley InterScience (www.interscience.wiley.com).

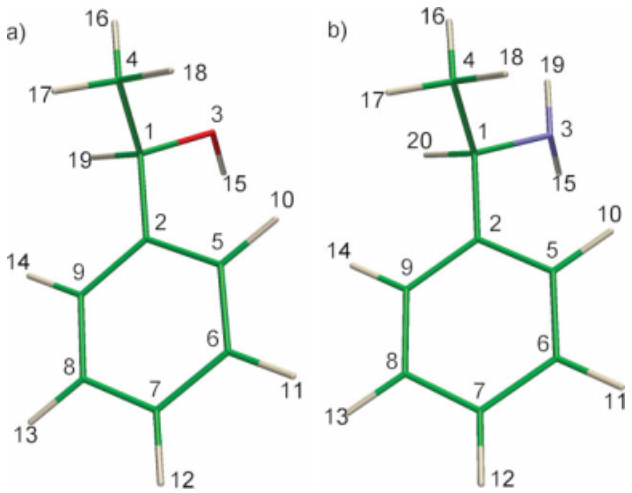

Fig. 1. Molecular structures of (+)-(*R*)-1-phenylethanol (**a**) and (+)-(*R*)-1-phenyethylamine (**b**). The torsion angles used to rotate the three functional groups of the compounds are defined as follows: phenyl rotation around C5-C2-C1-C4; methyl rotation around H16-C4-C1-C2; hydroxyl rotation around H15-O3-C1-C4; and amine rotation around H15-N3-C1-C2. [Color figure can be viewed in the online issue, which is available at www.interscience.wiley.com.]

origins of the first reported ROA signals. The influence of conformational averaging is considered in detail, together with estimates of the effects of anharmonicity.

MATERIALS AND METHODS

Samples of (+)-(*R*)- and (−)-(*S*)-1-phenylethanol and (+)-(*R*)- and (−)-(*S*)-1-phenylethylamine were supplied by Lancaster Synthesis (Alfa Aesar) and were studied as neat liquids. SCP ROA spectra were measured in backscattering using the previously described ChiralRAMAN instrument (BioTools).[4] The ROA spectra are presented as $I_R - I_L$ and the parent Raman spectra as $I_R + I_L$, where I_R and I_L are the Raman-scattered intensities with right- and left-circular polarization, respectively. The normalized circular intensity difference (CID), defined as $(I_R - I_L)/(I_R + I_L)$, is a dimensionless quantity useful for comparing experimental with calculated ROA band intensities. The experimental conditions were as follows: laser wavelength 532 nm; laser power at the sample ~20 mW; spectral resolution ~10 cm^{-1}; acquisition times ~140 min.

The quantum–chemical simulations of the Raman and ROA spectra were performed on the (+)-(*R*)- enantiomers using the Gaussian suite of programs.[10] The potential energy surfaces (PESs) of the two compounds were explored by rotating the phenyl and —OH or —NH_2 groups by increments of 10°, generating 648 unique structures for geometry optimization. In analyzing the PESs generated by the optimized structures, a cut-off at 3 kcal/mol was enforced before force field and tensor computations, reducing the number of conformations to 431 in the case of 1-phenylethanol and 343 in the case of 1-phenylethylamine.

To investigate the effects of methyl rotations when compared with phenyl and —OH or —NH_2 rotations, three different energy conformations were selected from each PES. Each optimized structure was subsequently used as the basis for a 10° incremental rotation of the methyl group, covering a 120° period and generating 12 new conformations for each of the starting structures, for which force fields and tensors were subsequently calculated.

All structural optimizations and force field calculations were performed at the B3LYP/6-311++G**/vacuum level, while the polarizability and optical activity tensor computations were performed at the HF/rDPS[11]/vacuum level. In practical terms, the HF methods provide very similar spectral intensities to B3LYP but at significantly reduced computational cost.[5,12,13] The Raman and ROA spectra were subsequently simulated within the harmonic approximation using the usual procedure.[14]

Anharmonic corrections, carried out on the lowest energy conformation of 1-phenylethanol, were calculated employing the program S4[15] interfaced with Gaussian.[10] The calculations involved third- and semi-diagonal (d_{iijk}) fourth-energy derivatives and second polarizability derivatives obtained by numerical differentiation from the second energy and first polarizability derivatives.[12,16–19] The differentiation was done both in the Cartesian and normal mode coordinates, with Cartesian step of 0.05 Å or normal mode displacement corresponding approximately to this value. As the two differentiation procedures provided very similar spectra, only the normal mode results are reported. Only first derivatives of the ROA $\mathbf{G}'$ and $\mathbf{A}$ tensors were used, as obtained at the HF/rDPS (local parts) and B3LYP/6-311++G** (reducible polarizability part) levels.

Three different anharmonic correction methods were applied: vibrational self-consistent field (VSCF),[20] second-order perturbation calculus (PT2) with the random-degeneracy corrected formula,[12,19] and a limited vibrational configuration interaction (VCI). The harmonic oscillator basis was used, with harmonic spectral intensities in VSCF and PT2. To achieve numerical stability in the VCI calculations,[19] 35,408 states were required, with excitations of the nine lowest energy normal modes excluded.

RESULTS AND DISCUSSION

Comparison of Experimental and Simulated Spectra

The top panels, (a) and (d), in Figure 2 display the experimental backscattered Raman and ROA spectra of both enantiomers of 1-phenylethanol and 1-phenylethylamine, respectively. All the presented data are for the (+)-(*R*)-enantiomers, except for the experimental ROA spectra for which data from both enantiomers are shown. The ROA spectra of the two enantiomers of the alcohol exhibit almost perfect mirror-image symmetry, but some small deviations from perfect mirror-image symmetry exist for several of the ROA bands of the amine enantiomers associated with strongly polarized parent Raman bands (which, as was appreciated at the time of the first observations, can be susceptible to instrumental artifacts[1]). These small differences persisted during several repeated measurements despite careful distillation of the samples and also while measuring different batches of samples from a different supplier (Sigma Aldrich). The middle panels (b) and

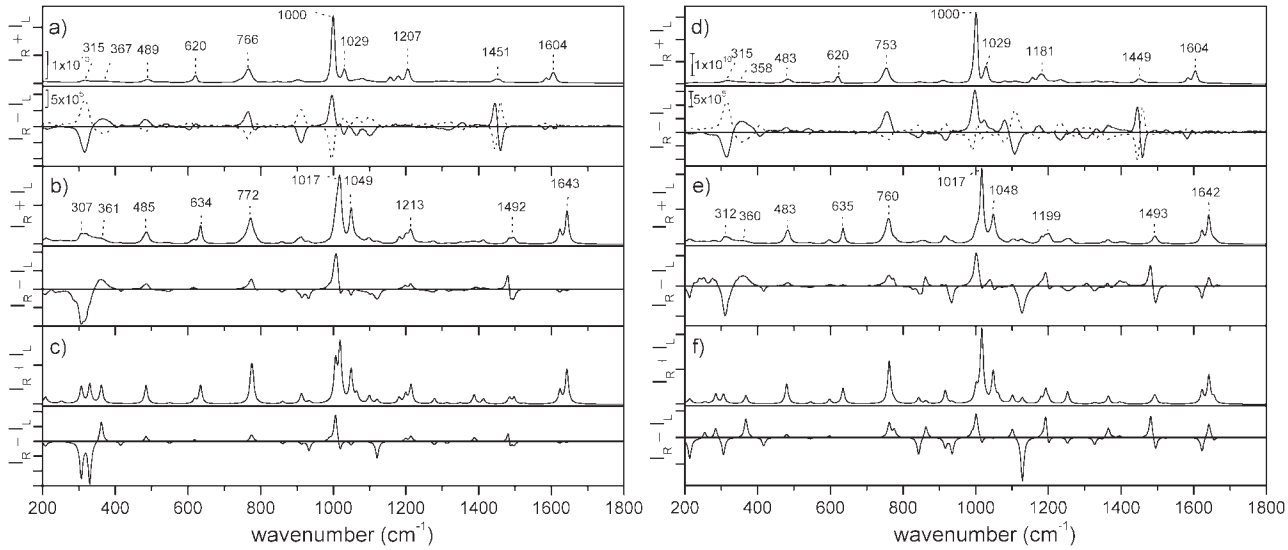

Fig. 2. Comparison of experimental and simulated Raman ($I_R + I_L$) and ROA ($I_R - I_L$) spectra of (**a–c**) 1-phenylethanol and (**d–f**) 1-phenyethylamine. (a, d) experimental spectra, (**b**, **e**) Boltzmann average of simulated spectra, (c, f) single geometry spectra of lowest energy conformations. All data shown are for the (+)-(*R*)-enantiomers, except for the experimental ROA spectra, where spectra of both the (+)-(*R*)- and (−)-(*S*)-enantiomers are displayed as solid and dotted lines, respectively. The (b, e) simulated spectra were calculated for all conformations below 3 kcal/mol, 431 structures in the case of the alcohol and 343 structures in the case of the amine.

(e) in Figure 2 display the corresponding simulated Raman and ROA spectra. For many molecules, it is necessary to allow some degree of conformational freedom to simulate the observed Raman and ROA bandshapes more realistically.[6,13,21] In this case, to achieve a closer agreement between the calculated and experimental ROA spectra, it was necessary to take a Boltzmann average over rotameric conformations of the phenyl and —OH or —NH_2 groups. The bottom panels (c) and (f) display the corresponding simulated spectra for a single lowest energy conformation only. It is clear that the single conformation bands are too sharp and strong, the calculated ROA spectra being reminiscent of those observed in enantiomorphous crystals where in particular the rotational freedom around single bonds is suppressed.[22] For the same reason, an earlier fixed-geometry simulation of the ROA spectrum of (+)-(*R*)-1-phenylethanol similarly generated some bands that were too sharp and strong.[23]

Although measured in SCP backscattering, rather than in ICP depolarized right-angle scattering as in the original report,[1] similar ROA couplets in the spectral range ~280–400 cm^{-1} are observed. This observation may be

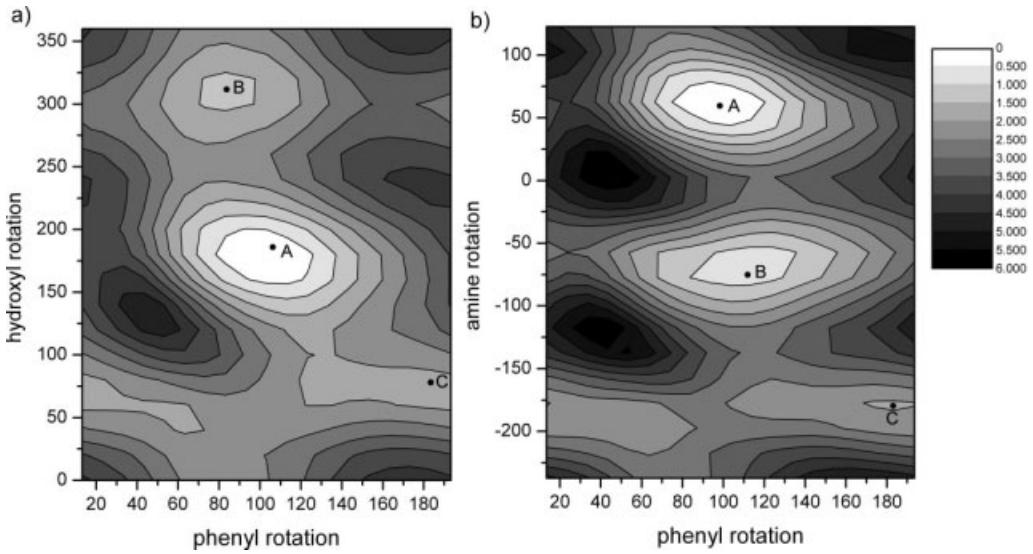

Fig. 3. Two-dimensional PESs of (+)-(*R*)-1-phenylethanol (**a**) and (+)-(*R*)-1-phenyethylamine (**b**) (kcal/mol). Scanning of the PES was accomplished by rotating the phenyl and —OH or —NH_2 groups in 10° steps. The methyl group was rotated independently of the other two rotations, employing an energy barrier ~4 kcal/mol. The three positions marked A, B, and C correspond to the starting conformations for one-dimensional potential energy scans of the methyl rotation in Figure 6.

explained by the fact that in both experimental configurations only purely anisotropic molecular property tensor invariants contribute to the ROA intensities.[24]

Influence of Conformational Averaging on Band Widths and Intensities

Figure 3 displays the PESs of 1-phenylethanol and 1-phenylethylamine, plotted as a function of phenyl and —OH or $—NH_2$ rotations, respectively. Over the total scanned surface, the potential energy of the alcohol varies within ~5 kcal/mol, while the amine reaches ~6 kcal/mol above the global minimum. Both compounds exhibit a single (global) minimum and several energy-close local minima; thus, many conformations are expected to be present and must be included in the modeling. The percentage weights of the conformational contributions of both compounds with respect to conformer energies are presented in Figure 4. Each column represents a 0.5 kcal/mol interval, hence illustrating that, even though the low energy conformations contribute significantly to the Boltzmann distribution, conformations with energies above 1 kcal/mol still account for ~40% of the total weighted average.

Additionally, Figure 4 also shows that the contributions to the final weighted average do not necessarily decrease uniformly with increasing energy. Comparing the 1.5–2.0 kcal/mol column with the 1.0–1.5 kcal/mol column in the case of 1-phenylethanol, for example, the increase in percentage contribution can be accounted for by the sheer number of conformations present in the higher energy interval, namely, 100 conformations compared with 32 in the lower energy interval.

Although each conformation will contribute very little to the final averaged spectrum, the inclusion of a full set of conformations evidently improves the final result, especially with regard to the band width and relative band intensities of the averaged spectra. Figure 5 compares the contribution to shape and intensity with respect to conformational energy for both Raman and ROA spectra. Although Figures 5a and 5c show that similar contributions to the Raman band intensities are supplied by the low- and high-energy conformations in the case of both compounds, the contributions to ROA decrease significantly with increasing energy. This difference in behavior of Raman and ROA spectra is important if direct comparison between experimental and simulated Raman and ROA spectra is required, especially when comparing CID values, and is also a useful illustration of the distinct difference in contributions to the polarizability and optical activity tensors from different conformations.

Table 1 lists the CID values for some selected individual bands, comparing experimental values with values calculated from simulated data generated from the Boltzmann-weighted spectra containing all conformations and also from the simulated spectra of the 50% lowest energy conformations. The CIDs compare reasonably well, being of the same order of magnitude, except for the strongly polarized band measured at ~1000 cm^{-1} in 1-phenylethanol. This discrepancy is due to an underestimation of the simulated Raman intensity of this band, which could be explained by the limitations imposed by the choice of basis set, as the ~1000 cm^{-1} band can be assigned to mainly aromatic carbon–carbon stretching vibrations in the phenyl ring, whereas the rDPS basis set only employs a minimal set of carbon p-type basis functions. Surprisingly, the CID values of the corresponding band in 1-phenylethylamine compare much better, indicating that the discrepancy in the case of the alcohol may not be entirely due to the limited basis set. It is also evident from Table 1 that the two CIDs calculated for the BBB couplets increase in value as the number of energy conformations decreases, illustrating that the corresponding spectral region is highly sensitive to conformational averaging.

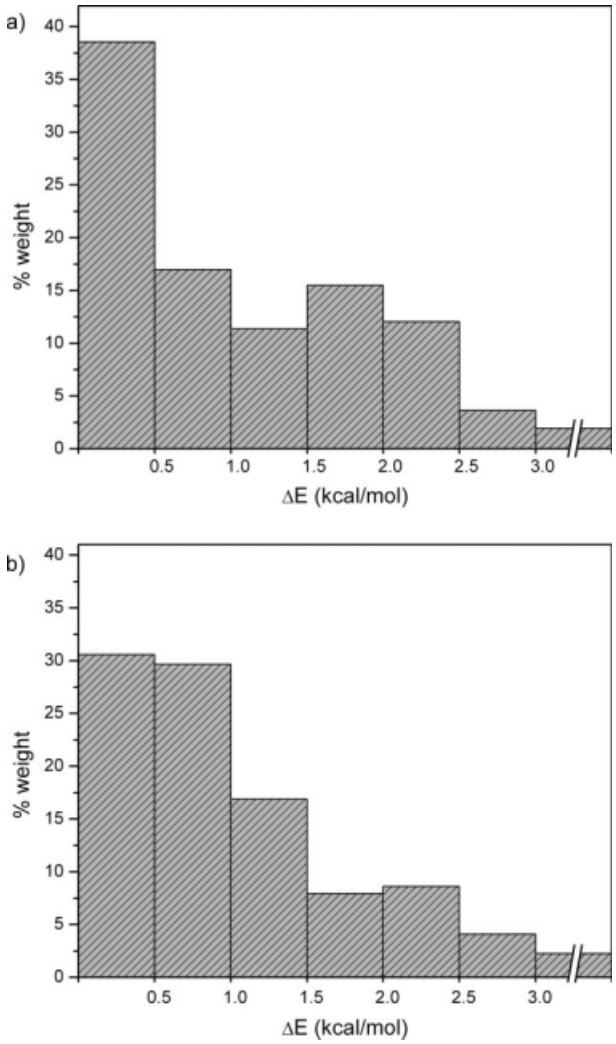

Fig. 4. Percentage distribution of the Boltzmann-averaged conformations with respect to potential energy (kcal/mol) of (+)-(*R*)-1-phenylethanol (**a**) and (+)-(*R*)-1-phenyethylamine (**b**).

Before the PES scanning calculations, we assumed that rotation of the methyl group in 1-phenylethanol and 1-phenylethylamine is isolated from rotations of the other two functional groups, and would therefore have only limited influence on the appearance of the simulated spectra. To verify this hypothesis, three single conformations were chosen from the PES of both compounds and subjected to a one-dimensional potential energy scan, merely rotating

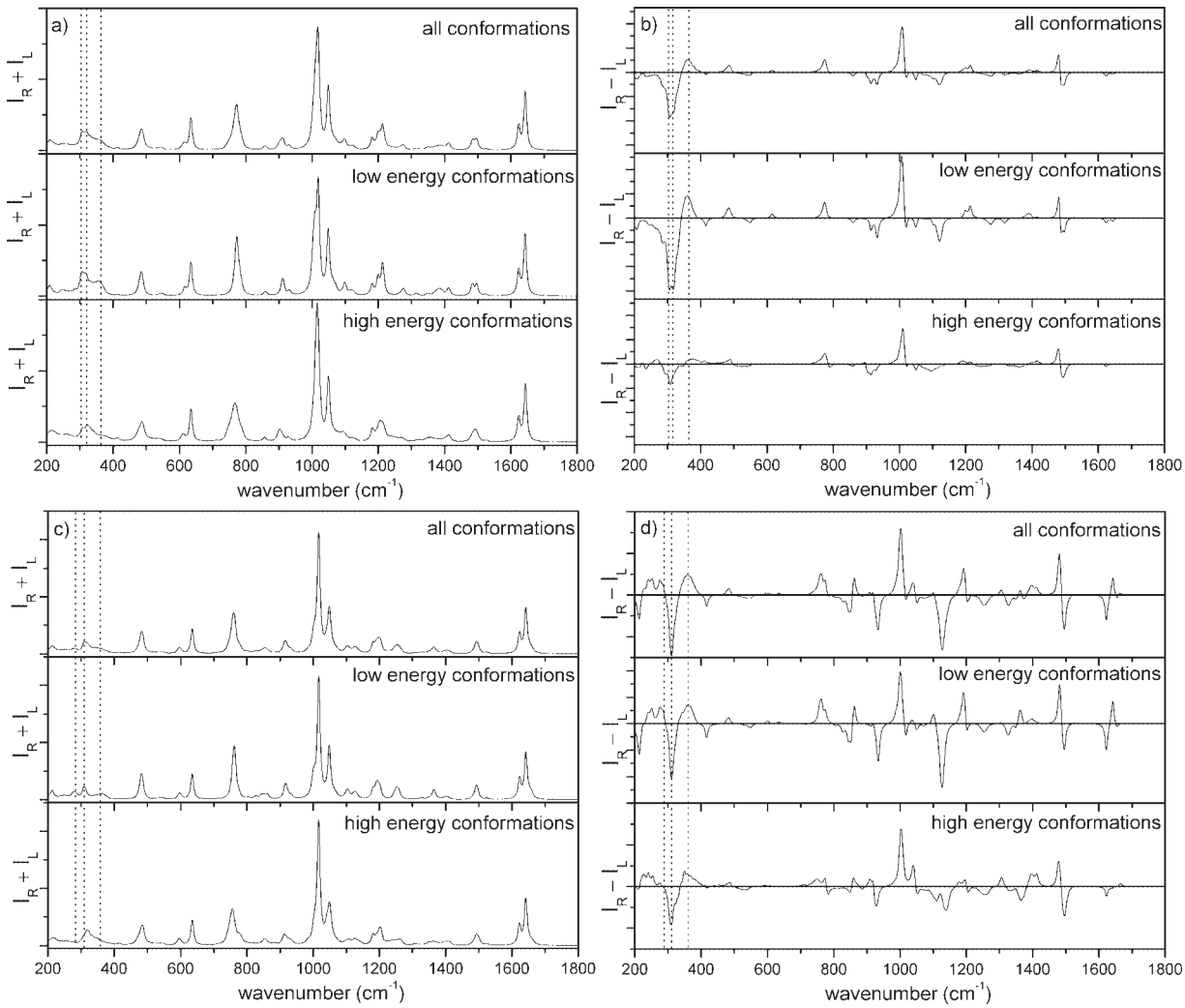

Fig. 5. Simulated Boltzmann-averaged spectra of (+)-(*R*)-1-phenylethanol (**a**, **b**) and (+)-(*R*)-1-phenyethylamine (**c**, **d**), comparing the Raman (a, c) and ROA (b, d) spectra averaged over all conformations (top spectra) with the band intensities contributed by low energy conformations (50% contribution, 0–0.8 kcal/mol, middle spectra) and high energy conformations (50% contribution, >0.8–3 kcal/mol, bottom spectra). Each set of spectra is plotted using the same intensity range to visualize the different contributions. The positions of the BBB couplet modes are indicated with dotted lines.

the methyl group. These three conformations were, for both the alcohol and the amine, the global energy minimum (point A), a local minimum (point B), and a higher energy conformation (point C). The positions of each conformation in the PESs of the two compounds are shown in Figure 3. Figure 6 displays the normalized potential

TABLE 1. CID values for selected individual bands in the experimental and simulated spectra of (+)-(*R*)-1-phenylethanol and (+)-(*R*)-1-phenylethylamine

(+)-(*R*)-1-phenylethanol				(+)-(*R*)-1-phenylethylamine			
Band (cm^{-1})	Exp.[a] CID × 10^4	Sim. all confs.[b] CID × 10^4	Sim. lowest confs.[c] CID × 10^4	Band (cm^{-1})	Exp.[a] CID × 10^4	Sim. all confs.[b] CID × 10^4	Sim. lowest confs.[c] CID × 10^4
315	−6.9	−10.3	−12.7	315	−6.2	−6.8	−9.3
367	3.1	5.1	6.7	358	4.8	5.2	6.8
766	0.9	1.2	1.2	753	1.0	0.7	1.0
1000	0.3	1.3	1.5	1000	0.5	0.7	0.6
1029	−0.5	−0.5	−0.6	1029	0.4	0.3	0.2
1451	1.0	1.9	1.5	1449	1.1	1.6	1.6

[a]Experimental CIDs at the measured frequencies.
[b]Simulated CIDs based on all conformations.
[c]Simulated CIDs based on the 50% lowest-energy conformations.

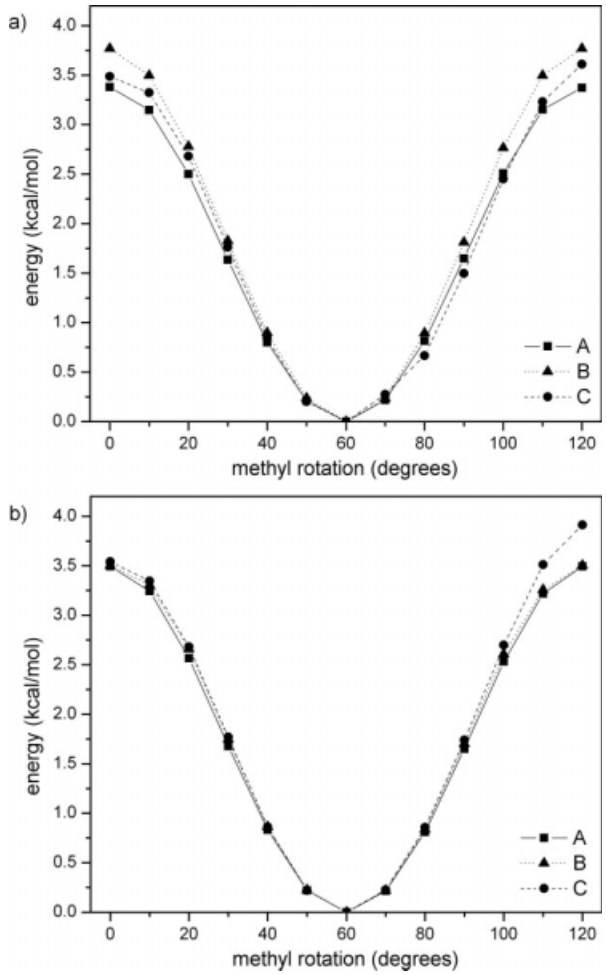

Fig. 6. Potential energy curves illustrating the energy dependence of methyl rotations in (+)-(*R*)-1-phenylethanol (**a**) and (+)-(*R*)-1-phenyethylamine (**b**). The three curves (A, B, and C) displayed in each graph originate from separate potential energy scans, using three different starting structures extracted from the PES based on phenyl and $-OH$ or $-NH_2$ rotations.

energy curves obtained by performing these scans. As the curves are virtually identical, both in the case of the alcohol and the amine, rotation of the methyl group is indeed isolated from rotations of the two other groups. Calculated spectra of optimized structures with different methyl group rotations revealed only minor changes in comparison to the corresponding spectra of the original conformations (A, B, or C).

Normal Mode Contributions to the BBB Couplets

The detailed conformational analysis of 1-phenylethanol and 1-phenylethylamine permits the assignment of the normal mode vibrations contributing to the broad BBB ROA couplets that constituted the first observations of vibrational optical activity.[1] Graphical representations of the three normal modes making the major contributions to the BBB couplets of both compounds, using the global minimum structures as examples, are depicted in Figure 7. In the case of 1-phenylethanol, these normal modes comprise coupled methyl and phenyl ring deformations (the 305 cm^{-1} mode), an isolated —OH torsion (the 315 cm^{-1} mode), and a coupled —OH torsion and methyl deformation (the 362 cm^{-1} mode). Additionally, a methyl torsion normal mode contributes to a minor degree. In 1-phenylethylamine, the three normal modes comprise an out-of-phase combination of methyl and $-NH_2$ torsions (the 285 cm^{-1} mode), coupled methyl and phenyl ring deformations (the 312 cm^{-1} mode, similar to the 305 cm^{-1} mode in the alcohol) and a coupled $-NH_2$ torsion and methyl deformation (the 360 cm^{-1} mode, similar to the 362 cm^{-1} mode in the alcohol). There is also a minor contribution from an in-phase combination of methyl and $-NH_2$ torsions. The broad appearance of the experimental BBB couplet results from the variations in frequency, intensity, and even sign of the ROA bands associated with normal modes in the corresponding spectral range from the plethora of other conformations in addition to the lowest energy conformations to which the normal modes depicted in Figure 7 pertain.

Anharmonic Corrections

Although conformational averaging improves the CID values of the ROA bands together with the shapes of the Raman and ROA bands within the simulated spectra, the harmonic approximation limits the accuracy of the calculated frequencies. To estimate the anharmonic corrections, anharmonic Raman spectra for a single geometry of 1-phe-

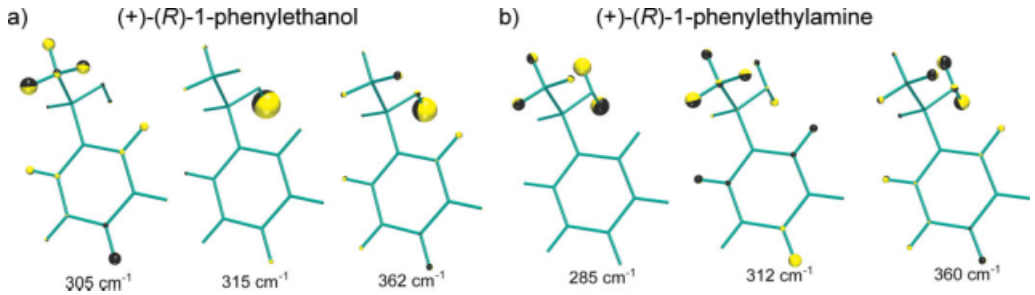

Fig. 7. Sketches of the three normal modes providing the major contributions to the BBB ROA couplet for (+)-(*R*)-1-phenylethanol (**a**) and (+)-(*R*)-1-phenylethyamine (**b**). Each sphere represents an atomic displacement vector, with the direction of the displacement perpendicular to the plane at the hemisphere junction, while the radius of the sphere represents the displacement amplitude. These normal modes are derived from calculations based on the lowest energy conformations, produced using the Pyvib visualization program.[25] [Color figure can be viewed in the online issue, which is available at www.interscience.wiley.com.]

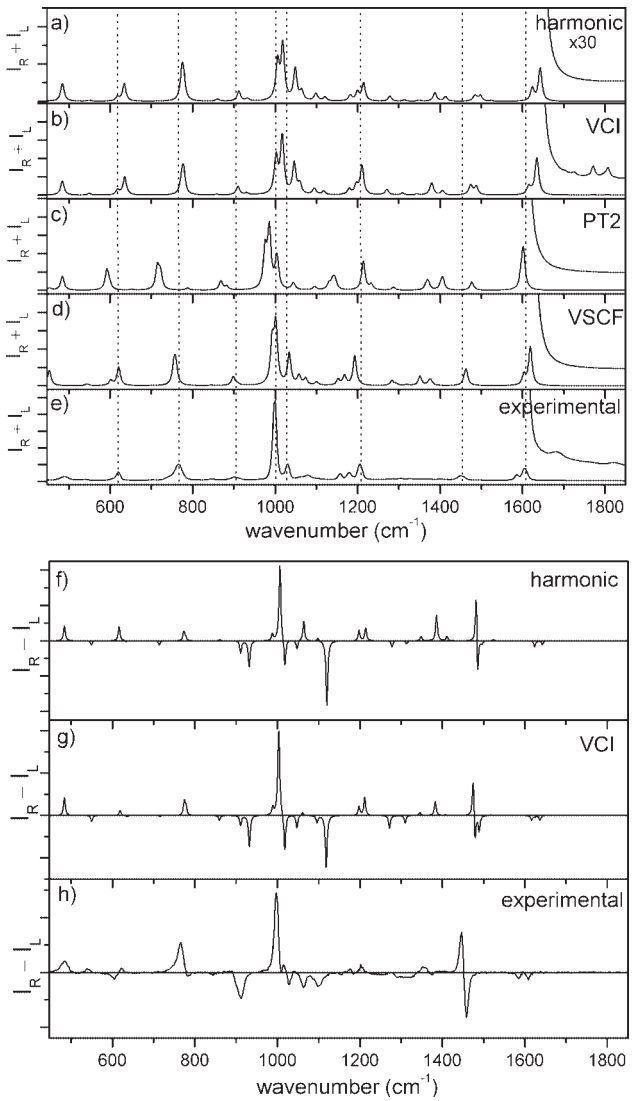

Fig. 8. Effects of anharmonic corrections to the simulated Raman and ROA spectra of the lowest-energy conformation of (+)-(*R*)-1-phenylethanol. The upper panel compares the harmonic (**a**), VCI-corrected (**b**), PT2-corrected (**c**), and VSCF-corrected (**d**) Raman spectra. The experimental spectrum (**e**) is shown at the bottom. Major bands are marked with dotted lines, and the wavenumber region 1650–1850 cm^{-1} has been magnified 30 times in each spectrum to expose the combination bands. In the lower panel, the harmonic (**f**), VCI (**g**), and experimental (**h**) ROA spectra are compared. The frequency range was reduced to 447–1850 cm^{-1} in this figure as low frequency modes were not included in the VCI calculation.

nylethanol were simulated as presented in the top panel of Figure 8.

In spite of the limited Taylor expansion of the potential energy and other approximations used, we can see that all three VCI, PT2, and VSCF anharmonic methods generated reasonable energy corrections to the harmonic case for the medium and higher-frequency vibrations (above ~1000 cm^{-1}). Trial computations indicate that the corrections are relatively insensitive to the fixing of the lowest-energy vibrations, which suggests that it may be partially possible also to adiabatically separate the lower and higher frequency motions in an anharmonic approach. The PT2 and to some extent also the VSCF method somewhat overestimates the corrections below ~1200 cm^{-1}, providing frequencies that were too low compared to the experimental results. The PT2 and VSCF computations, where more excited states could be involved, provide better simulations of the experimental bands at ~1450 and ~1000 cm^{-1}. On the other hand, VCI appears to be more appropriate for the region above ~1500 cm^{-1}, where it provides at least qualitatively correct anharmonic intensities observable in the range ~1600–1900 cm^{-1} in the higher-frequency wing of the fundamental ~1600 cm^{-1} band.

Simulation of the anharmonic ROA intensities (bottom panel of Fig. 8) by the VCI method also led to minor improvements compared to the harmonic case, while PT2 and VSCF anharmonic ROA intensities are virtually identical to the harmonic ones and therefore are not shown. The couplet at ~616/636 cm^{-1} is in both approximations calculated with the wrong signs, but the ROA intensity at least becomes smaller for VCI. The negative ROA signal at 714 cm^{-1} and the positive signal at 1064 cm^{-1} decrease in intensity, thus increasing the similarity to the experimental ROA spectrum. The signs of the very weak harmonic ROA bands at 858 and 1099 cm^{-1} are reversed by VCI, again in better agreement with experiment. The harmonic negative ROA signal at 1485 cm^{-1} becomes unrealistically split into two components (1480 and 1490 cm^{-1}) in VCI, but the overall intensity increase of this signal is in agreement with experiment, where the negative lobe of the couplet centered at ~1451 cm^{-1} is the more intense.

CONCLUSIONS

This study has demonstrated how easy and routine ROA measurements have become, and how current ab initio quantum–chemical calculations are able to simulate the experimental ROA spectrum quite closely provided sufficient averaging over accessible conformations is included. As with the complementary technique of vibrational circular dichroism (VCD),[26] assignments of absolute configurations (inter alia) are completely secure from ROA results of this quality.[6,11] Even the earliest ab initio simulations of ROA spectra, initiated 20 yrs ago,[27,28] produced reliable absolute configurations, exemplified by the first assignment for CHFClBr, which was inaccessible to other methods at the time.[29] However, with the increasing precision of measurements and calculations, there is a need to account for finer molecular dynamics and even anharmonic effects to achieve further improvements in simulations of ROA spectra.

VCD calculations are currently more economical than ROA calculations. However, ROA measurements may be performed more readily on samples in aqueous solution and over a much wider spectral range. Implementation of analytical, in place of the current numerical, calculations of the required property tensor derivatives should significantly speed up the routine simulation of ROA spectra.[7] In general, conformational averaging is expected to be even more important for ROA calculations than for VCD calculations[26] because ROA spectra penetrate well below the cur-

rent ~800 cm^{-1} cut-off of VCD spectra, where the normal modes are increasingly sensitive to conformational changes and hence conformer populations.

The much greater sensitivity of ROA to conformational freedom than conventional Raman, demonstrated analytically via ab initio simulations in this and in previous recent studies,[13,21] was already noticed qualitatively some years ago from experimental studies on biomolecules such as proteins and nucleic acids.[30] For example, it was appreciated that the remarkable sensitivity of ROA to dynamic aspects of biomolecular structure was because of the fact that, because ROA observables depend on absolute chirality, there is a cancellation of contributions with opposite signs from quasi-enantiomeric structures, which can result as mobile structure explores the range of accessible conformations.[30] This characteristic of ROA has been exploited in numerous studies of peptide and protein structure and behavior.[31,32] As well as order-to-disorder (and vice versa) transitions of the peptide backbone, amino acid sidechains are also valuable probes of conformational changes. For example, the ~1545–1560 cm^{-1} tryptophan ROA band, assigned to a W3-type vibration of the indole ring, has been used to determine the absolute stereochemistry of the tryptophan conformation in proteins, the original qualitative interpretation[33] having recently been verified by ab initio simulations.[34] But in addition, the W3 band is a valuable probe of conformational heterogeneity among a set of tryptophans in disordered sequences because cancellation from ROA contributions with opposite signs can result in a dramatic loss of ROA intensity, examples being observed in transitions from native-to-molten globule states of equine lysozyme and human lysozyme.[31,32] The importance of conformational averaging emphasized by the work reported here provides the underlying theoretical background to ROA studies of dynamic aspects of chiral molecular and biomolecular structure and behavior.

LITERATURE CITED

1. Barron LD, Bogaard MP, Buckingham AD. Raman scattering of circularly polarized light by optically active molecules. J Am Chem Soc 1973;95:603–605.
2. Hug W, Kint S, Bailey GF, Scherer JR. Raman circular intensity differential spectroscopy. The spectra of (−)-α-pinene and (+)-α-phenylethylamine. J Am Chem Soc 1975;97:5598–5590.
3. Hug W. Raman optical activity. In: Chalmers JM, Griffiths PR, editors. Handbook of vibrational spectroscopy, Vol. 1. Chichester: Wiley; 2002. p 745–758.
4. Barron LD, Zhu F, Hecht L, Tranter GE, Isaacs NW. Raman optical activity: an incisive probe of molecular chirality and biomolecular structure. J Mol Struct 2007;834–836:7–16.
5. Pecul M, Ruud K. Ab initio calculation of vibrational Raman optical activity. Int J Quantum Chem 2005;104:816–829.
6. Haesler J, Schindelholz I, Riguet E, Bochet CG, Hug W. Absolute configuration of chirally deuterated neopentane. Nature 2007;446:526–529.
7. Liégeois V, Ruud K, Champagne B. An analytical derivative procedure for the calculation of vibrational Raman optical activity spectra. J Chem Phys 2007;127:204105.
8. Kapitán J, Zhu F, Hecht L, Gardiner J, Seebach D, Barron LD. Solution structure of β-peptides from Raman optical activity. Angew Chem Int Ed 2008;47:6392–6394.
9. Nafie LA. Theory of Raman scattering and Raman optical activity: near resonance theory and levels of approximation. Theor Chem Acc 2008;119:39–55.
10. Frisch MJ, Trucks GW, Schlegel HB, Scuseria GE, Robb MA, Cheeseman JR, Montgomery Jr JA, Vreven T, Kudin KN, Burant JC, Millam JM, Iyengar SS, Tomasi J, Barone V, Mennucci B, Cossi M, Scalmani G, Rega N, Petersson GA, Nakatsuji H, Hada M, Ehara M, Toyota K, Fukuda R, Hasegawa J, Ishida M, Nakajima T, Honda Y, Kitao O, Nakai H, Klene M, Li X, Knox JE, Hratchian HP, Cross JB, Bakken V, Adamo C, Jaramillo J, Gomperts R, Stratmann RE, Yazyev O, Austin AJ, Cammi R, Pomelli C, Ochterski JW, Ayala PY, Morokuma K, Voth GA, Salvador P, Dannenberg JJ, Zakrzewski VG, Dapprich S, Daniels AD, Strain MC, Farkas O, Malick DK, Rabuck AD, Raghavachari K, Foresman JB, Ortiz JV, Cui Q, Baboul AG, Clifford S, Cioslowski J, Stefanov BB, Liu G, Liashenko A, Piskorz P, Komaromi I, Martin RL, Fox DJ, Keith T, Al-Laham MA, Peng CY, Nanayakkara A, Challacombe M, Gill PMW, Johnson B, Chen W, Wong MW, Gonzalez C, Pople JA. Gaussian 03, Revision D.02. Wallingford CT: Gaussian, Inc.; 2004.
11. Zuber G, Hug W. Rarefied basis sets for the calculation of optical tensors. 1. The importance of gradients of hydrogen atoms for the Raman scattering tensor. J Phys Chem A 2004;108:2108–2118.
12. Daněček P, Kapitán J, Baumruk V, Bednárová L, Kopecký V Jr., Bouř P. Anharmonic effects in IR, Raman, and Raman optical activity spectra of alanine and proline zwitterions. J Chem Phys 2007;126:224513.
13. Kapitán J, Baumruk V, Kopecký V Jr, Pohl R, Bouř P. Proline zwitterionic dynamics in solution, glass and crystalline state. J Am Chem Soc 2006;128:13451–13462.
14. Nafie LA, Che D. Theory and measurement of Raman optical activity. In: Evans M, Kielich S, editors. Modern nonlinear optics, Part 3, Vol. 85. New York: Wiley; 1994. p 105–149.
15. Bouř P. S4. Academy of Sciences. Prague: Prague; 2009.
16. Barone VJ. Anharmonic vibrational properties by a fully automated second-order perturbative approach. J Chem Phys 2005;122:014108.
17. Bouř P. Anharmonic corrections to vibrational energies of molecules: water and dideuteriooxirane. J Phys Chem 1994;98:8862.
18. Bouř P, Bednárová L. Anharmonic force field of formamide. A computational study. J Phys Chem 1995;99:5961–5966.
19. Daněček P, Bouř P. Comparison of the numerical stability of methods for anharmonic calculations of vibrational molecular energies. J Comput Chem 2007;28:1617–1624.
20. Brauer B, Chaban GM, Gerber RB. Spectroscopically-tested, improved, semi-empirical potentials for biological molecules: calculations for glycine, alanine and proline. Phys Chem Chem Phys 2004;6:2543–2556.
21. Kapitán J, Baumruk V, Kopecký V Jr, Bouř P. Conformational flexibility of L-alanine zwitterion determines shapes of Raman and Raman optical activity spectral bands. J Phys Chem A 2006;110:4689–4696.
22. Lindner M, Schrader B, Hecht L. Raman optical activity of enantiomorphous single crystals. J Raman Spectrosc 1995;26:877–882.
23. Macleod NA, Butz P, Simons JP, Grant GH, Baker CM, Tranter GE. Structure, electronic circular dichroism, and Raman optical activity in the gas phase and in solution: a computational and experimental investigation. Phys Chem Chem Phys 2005;7:1432–1440.
24. Barron LD. Molecular light scattering and optical activity, 2nd ed. Cambridge: Cambridge University Press; 2004.443 p.
25. Fedorovsky M. Exploring vibrational optical activity with PyVib2. Comp Lett 2006;2:233–236.
26. Stephens PJ, Devlin FJ, Pan JJ. The determination of absolute configuration of chiral molecules using vibrational circular dichroism (VCD) spectroscopy. Chirality 2008;20:643–663.
27. Bose PK, Barron LD, Polavarapu PL. Ab initio and experimental vibrational Raman optical activity in (+)-(R)-methylthiirane. Chem Phys Lett 1989;155:423–429.
28. Polavarapu PL. Ab initio vibrational Raman and Raman optical activity spectra. J Phys Chem 1990;94:8106–8112.

29. Costante J, Hecht L, Polavarapu PL, Collet A, Barron LD. Absolute configuration of bromochlorofluoromethane from experimental and ab initio theoretical vibrational Raman optical activity. Angew Chem Int Ed Engl 1997;36:885–887.
30. Barron LD, Hecht L, Blanch EW, Bell AF. Solution structure and dynamics of biomolecules from Raman optical activity. Prog Biophys Mol Biol 2000;73:1–49.
31. Barron LD, Blanch EW, Hecht L. Unfolded proteins studied by Raman optical activity. Adv Prot Chem 2002;62:51–90.
32. Barron LD, Zhu F, Hecht L, Isaacs NW. Structure and behavior of proteins from Raman optical activity. In: Uversky VN, Permyakov EA, editors. Methods in protein structure and stability analysis. New York: Nova Science Publishers; 2007. p 27–68.
33. Blanch EW, Hecht L, Day LA, Pederson M, Barron LD. Tryptophan absolute stereochemistry in viral coat proteins from Raman optical activity. J Am Chem Soc 2001;123:4863–4864.
34. Jacob CR, Luber S, Reiher M. Calculated Raman optical activity signatures of tryptophan side chains. Chem Phys Chem 2008;9:2177–2180.